



## **Ananke: A Streaming Framework for Live Forward Provenance**

Downloaded from: <https://research.chalmers.se>, 2025-12-04 14:42 UTC

Citation for the original published paper (version of record):

Palyvos-Giannas, D., Havers, B., Papatriantafilou, M. et al (2020). Ananke: A Streaming Framework for Live Forward Provenance. Proceedings of the VLDB Endowment, 14(3): 391-403.  
<http://dx.doi.org/10.14778/3430915.3430928>

N.B. When citing this work, cite the original published paper.

# Ananke: A Streaming Framework for Live Forward Provenance

Dimitris Palyvos-Giannas  
Chalmers Univ. of Technology  
Gothenburg, Sweden  
palyvos@chalmers.se

Marina Papatriantafylou  
Chalmers Univ. of Technology  
ptrianta@chalmers.se

Bastian Havers  
Chalmers Univ. of Technology, Volvo Car Corporation  
Gothenburg, Sweden  
havers@chalmers.se

Vincenzo Gulisano  
Chalmers Univ. of Technology  
vinmas@chalmers.se

## ABSTRACT

Data streaming enables online monitoring of large and continuous event streams in Cyber-Physical Systems (CPSs). In such scenarios, fine-grained backward provenance tools can connect streaming query results to the source data producing them, allowing analysts to study the dependency/causality of CPS events. While CPS monitoring commonly produces many events, backward provenance does not help prioritize event inspection since it does not specify if an event's provenance could still contribute to future results.

To cover this gap, we introduce *Ananke*, a framework to extend any fine-grained backward provenance tool and deliver a live bi-partite graph of fine-grained forward provenance. With *Ananke*, analysts can prioritize the analysis of provenance data based on whether such data is still potentially being processed by the monitoring queries. We prove our solution is correct, discuss multiple implementations, including one leveraging streaming APIs for parallel analysis, and show *Ananke* results in small overheads, close to those of existing tools for fine-grained backward provenance.

## PVLDB Reference Format:

Dimitris Palyvos-Giannas, Bastian Havers, Marina Papatriantafylou, and Vincenzo Gulisano. Ananke: A Streaming Framework for Live Forward Provenance. PVLDB, 14(3): 391 - 403, 2021.

doi:10.14778/3430915.3430928

## PVLDB Artifact Availability:

The source code, data, and/or other artifacts have been made available at <https://github.com/dmpalyvos/ananke>.

## 1 INTRODUCTION

Distributed, large, heterogeneous Cyber-Physical Systems (CPSs) like Smart Grids or Vehicular Networks [22] rely on online analysis applications to monitor device data. In this context, the data streaming paradigm [36] and the DataFlow model [2] enable the inspection of large volumes of continuous data to identify specific patterns [16, 28]. Streaming applications fit CPSs' requirements due to the high-throughput, low-latency, scalable analysis enabled by Stream Processing Engines (SPEs) [1, 4, 5, 8, 31] and their correctness guarantees, which are critical for sensitive analysis. Figure 1a

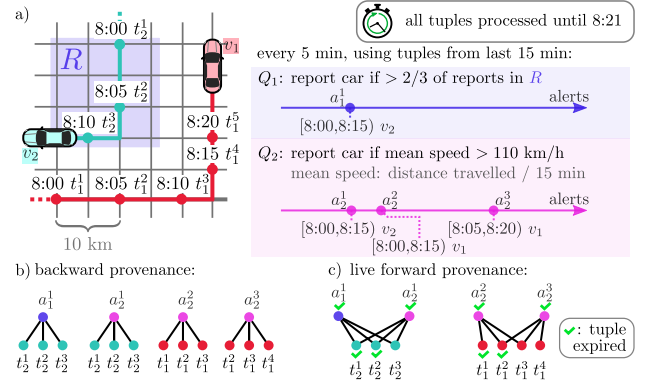


**Figure 1: a) Two sample queries to monitor car location and mean speed (all tuples up to time 8:21 are processed), and their b) backward and c) live forward provenance graphs.**

shows two streaming applications, or *queries*, monitoring a vehicular network to spot cars visiting a specific area ( $Q_1$ ) or speeding ( $Q_2$ ). Vehicle reports (timestamp, id, position), or *tuples*, arrive every 5 minutes;  $t_j^i$  is the  $i$ -th tuple from car  $j$ ,  $a_j^i$  the  $i$ -th alert from query  $j$ . This scenario is our running use-case throughout the paper.

**Motivating challenge.** CPSs need continuous monitoring for emerging threats or dangerous events [32, 37], which may result in many alerts that analysts are then left to prioritize [15, 34]. For streaming-based analysis, *provenance* techniques [19, 30], which connect results to their contributing data, are a practical way to inspect data dependencies, since breakpoint-based inspection is not fit for live queries that run in a distributed manner and cannot be paused [14]. Existing provenance tools for traditional databases target *backward tracing*, to find which source tuples contribute to a result [7, 11, 12, 14, 19] (Figure 1b), and *forward tracing*, to find which results originate from a source tuple [7, 12]; however, streaming-based tools only exist for backward-provenance [19, 30].

The need for live, streaming, forward provenance is multifold: (1) while backward tracing can give assurance on the trustworthiness of end-results [11], forward tracing allows to identify all results linked to specific inputs [12], e.g. to mark all results linked to a privacy-sensitive datapoint (e.g. a picture of a pedestrian, in the context of Vehicular Networks) before such results are analyzed further; (2) live maintenance of the provenance graph avoids data duplication and allows to start the analysis of provenance data safely (e.g., once all sensitive results that could be connected to the

This work is licensed under the Creative Commons BY-NC-ND 4.0 International License. Visit <https://creativecommons.org/licenses/by-nc-nd/4.0/> to view a copy of this license. For any use beyond those covered by this license, obtain permission by emailing [info@vldb.org](mailto:info@vldb.org). Copyright is held by the owner/author(s). Publication rights licensed to the VLDB Endowment.

Proceedings of the VLDB Endowment, Vol. 14, No. 3 ISSN 2150-8097.  
doi:10.14778/3430915.3430928

aforementioned picture have been marked); (3) a streaming-based forward provenance tool does not require intermediate disk storage (which might be forbidden for pictures taken in public areas) and enables lean dependency and causality analysis of the monitored events. Note that, as shown in our evaluation, providing live, streaming, forward provenance with tools external to the SPE running the monitoring queries incurs significant costs that can be avoided by relying on intra-SPE provenance processing instead.

**Contribution.** Motivated by the open issues, our key question is:

“Can we enrich data streaming frameworks that deliver backward provenance to efficiently provide live, duplicate-free, fine-grained, forward provenance for arbitrarily complex sets of queries?”

We answer affirmatively with our contributions:

- We formulate the concrete goals and evaluation metrics of solutions for live, duplicate-free, fine-grained, forward provenance.
- We implement a general framework, *Ananke*<sup>1</sup>, able to ingest backward provenance and deliver an evolving bipartite graph of live, duplicate-free, fine-grained, forward provenance (or simply live provenance) for arbitrary sets of queries. *Ananke* delivers each result and source tuple contributing to one or more results exactly once, distinguishing source data that could still contribute to more results from *expired* source data that cannot.
- *Ananke*’s key idea builds on our insights on forward provenance w.r.t. the backward provenance problem and defines a simple yet efficient approach, enabling specialized-operator-based implementations, as well as modular ones that utilize native operators of the underlying SPE. We design and prove the correctness of two streaming-based algorithmic implementations: one targeting to optimize the labeling of the expired source data as fast as possible, and one that shows how the general SPEs’ parallel APIs are sufficient to parallelize *Ananke*’s algorithm, and thus sustain higher loads of provenance data.
- We conduct a thorough evaluation of our *Ananke* implementation on top of Apache Flink [8], with real-world use cases and data, and also match with previous experiments and an implementation that delivers live forward provenance by relying on tools external to the SPE, for a fair comparison of *Ananke*’s overheads.

The implementations used in our evaluation are open-sourced at [18] for reproducibility. Figure 1c shows *Ananke*’s live provenance assuming both queries have processed all tuples up to time 8:21. Each source and sink tuple appear exactly once in the bipartite graphs. Some tuples are labeled by a green check-mark, indicating that they are expired and will not be connected to future results.

Organization: §2 covers preliminary data streaming and provenance concepts. §3 provides the definitions we use and also includes a formal problem formulation. §4-§5 cover our contribution, later evaluated in §6. We discuss related work in §7 and conclude in §8.

## 2 PRELIMINARIES

### 2.1 Data Streaming Basics

Like Apache Flink [8] (or simply Flink), *Ananke* builds on the DataFlow model [2]. *Streams* are unbounded sequences of *tuples*. Tuples have two *attributes*: the metadata  $\mu$  and the payload  $\phi$ , an array

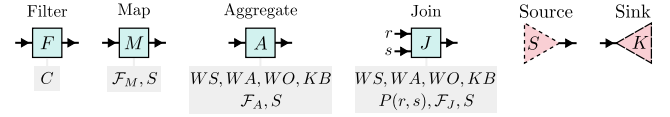


Figure 2: SPEs’ native operators, Source, and Sink.

of *sub-attributes*. The metadata  $\mu$  carries the timestamp  $\tau$  and possibly further sub-attributes. To refer to a sub-attribute of  $\mu$ , e.g.,  $\tau$ , we use the notation  $t.\tau$ . We reference  $\phi$ ’s  $i$ -th sub-attribute as  $t.\phi[i]$  (omitting  $t$  when it is clear from the context). In combined notation, a stream tuple is written as  $\langle \mu, \phi \rangle = \langle \tau, \dots, [\phi[1], \phi[2], \dots] \rangle$ .

*Streaming queries* (or simply queries) are composed of *Sources*, *operators* and *Sinks*. A Source forwards a stream of *source tuples* (e.g., events measured by a sensor or reported by other applications). Each *source stream* can be fed to one or more operators, the basic units manipulating tuples. Operators, connected in a Directed Acyclic Graph (DAG), process input tuples and produce output tuples; eventually, *sink tuples* are delivered to *Sinks*, which deliver results to end-users or other applications. In our model, we assume each tuple is immutable. Tuples are created by Sources and operators. The latter can also forward or discard tuples.

As source tuples correspond to events,  $\tau$  is set by the Source to when that event took place, the *event time*. Operators set  $\tau$  of each output tuple according to their semantics, while  $\phi$  is set by user-defined functions. Event time is not continuous but progresses in discrete increments defined by the SPE (e.g., milliseconds). We denote the smallest such increment of an SPE by  $\delta$ . All major SPEs [3–5, 8] support user-defined operators but also provide native ones: *Map*, *Filter*, *Aggregate* and *Join*. Since we make use of such native operators, we provide in the following their formal description for self-containment. However, *Ananke* provides live provenance without imposing any restriction on the operators of the query. Figure 2 illustrates the native operators, the Source, and the Sink. We begin with *stateless* operators, which process tuples one-by-one.

A **Filter (F)** relies on a user-defined filtering condition  $C$  to either forward an input tuple, when  $C$  holds, or discard it otherwise.

A **Map (M)** uses a user-defined function  $\mathcal{F}_M$  (to transform an input tuple into  $m \geq 1$  output tuples) and  $S$ , the schema of the output tuple payloads. It copies the  $\tau$  of each input into the outputs.

Differently from stateless operators, *stateful* ones run their analysis on *windows*, delimited groups of tuples maintained by the operators. *Time windows* are defined by their size  $WS$  (the length of the window), advance  $WA$  (the time difference between the left boundaries of consecutive windows), and offset  $WO$  (the alignment of windows relative to a reference time; in Flink, this is the Unix epoch). For example, a window having  $WS$ ,  $WA$ , and  $WO$  set to 60, 10 and 5 minutes, respectively, will cover periods [00:05,01:05), [00:15,01:15), etc. Consecutive periods covered by a window can overlap when  $WA < WS$ . Lastly, the left and right boundaries of a window are inclusive and exclusive, respectively. We say a tuple  $t$  falls in a window  $[A, B)$  if  $A \leq t.\tau < B$ . As windows can overlap, a tuple can fall into one or more windows.

We now present stateful operators in more detail.

An **Aggregate (A)** is defined by: (1)  $WS$ ,  $WA$ ,  $WO$ : the window size, advance, and offset, (2)  $KB$ : an optional key-by function to

<sup>1</sup>In Greek mythology, Ananke personifies inevitability, compulsion and necessity.

maintain separate (yet aligned) windows for different key-by values, (3)  $\mathcal{F}_A$ : a function to aggregate the tuples falling in one window into the  $\varphi$  attribute of the output tuple created for such window, (4)  $S$ : the output tuple's payload schema.

When an output tuple is created for a window (and a key-by value, if  $KB$  is defined), we assume its timestamp is set to such window's right boundary [3, 5, 8].

A **Join (J)** matches tuples from two input streams,  $r$  and  $s$ . It keeps two windows, one for  $r$  and one for  $s$  tuples, which share the same values for parameters  $WS$ ,  $WA$  and  $WO$ . Each pair of  $r$  and  $s$  tuples sharing a common key are matched for every pair of windows covering the same event-time period they fall in. The Join operator relies on the following parameters: (1)  $WS$ ,  $WA$ ,  $WO$ : the window size, advance, and offset, (2)  $KB$ : a key-by function to maintain separate (yet aligned) pairs of windows for different key-by values, (3)  $P(t_r, t_s)$ : a predicate for pairs of tuples from the two input streams, (4)  $\mathcal{F}_J$ : a function to create the  $\varphi$  attribute of the output tuple, for each pair of input tuples for which  $P(t_r, t_s)$  holds, and (5)  $S$ : the schema of the output tuple's payload  $\varphi$ . Similarly to the Aggregate, when an output tuple is created by a Join, its sub-attribute  $\tau$  is set to the right boundary of the window.

In the remainder, we (1) differentiate between stateless and stateful only if necessary, we (2) assume  $WO = 0$  unless otherwise stated, and (3) assume a stream can be multiplexed to many operators.

Figure 3 presents Figure 1's queries. Source  $S$  emits tuples of schema  $\langle \tau, [V_{id}, x, y] \rangle$  (timestamp, vehicle ID, x- and y-coordinates). In  $Q_1$ , Filter  $F_1$  forwards tuples within region  $R$ , Aggregate  $A_1$  counts each car's reports, and Filter  $F_2$  forwards to Sink  $K_1$  only tuples with a count higher than 2 (as tuples arrive every 5 minutes, the count can only be 1, 2 or 3). In  $Q_2$ , Aggregate  $A_2$  emits the mean speed of each car within the last 15 minutes. Filter  $F_3$  forwards the tuples whose mean speed<sup>2</sup> exceeds 110km/h to Sink  $K_2$ .

## 2.2 Watermarks and Correctness Guarantees

Because of asynchronous, parallel, and distributed execution, stateful operators processing tuples from multiple streams can receive such tuples out-of-order. Hence, receiving a tuple with a timestamp greater than some window's right boundary does not imply that tuples received later could not still contribute to said window.

To ensure result correctness for out-of-order streaming processing [25], Aggregate and Join rely on watermarks to make such distinction, as suggested by pioneer as well as state-of-the-art SPEs [8, 25]; the definition is paraphrased here:

**DEFINITION 2.1.** *The watermark  $W_i^\omega$  of operator  $O_i$  at a point in wall-clock time<sup>3</sup>  $\omega$  is the earliest event time a tuple to be processed by  $O_i$  can have from time  $\omega$  on (i.e.,  $t_i.\tau \geq W_i^\omega, \forall t_i$  processed from  $\omega$  on).*

Watermarks are created periodically by Sources and propagate as special tuples through the DAG<sup>4</sup>. Upon receiving a watermark, an operator stores the watermark's time, updates its watermark to the minimum of the latest watermarks received from each of

<sup>2</sup>In Figure 1, given the grid's cell size, cars' mean speed is 120km/h if covering four cells in three consecutive tuples.

<sup>3</sup>Notice that from here on, we only differentiate between wall-clock time (or simply time) and event time if such distinction is not clear from the context.

<sup>4</sup>Notice that this assumption about *in-band* watermarks is not a constraint. Different watermarking schemes that could also be adopted are discussed in e.g., [25, 26].

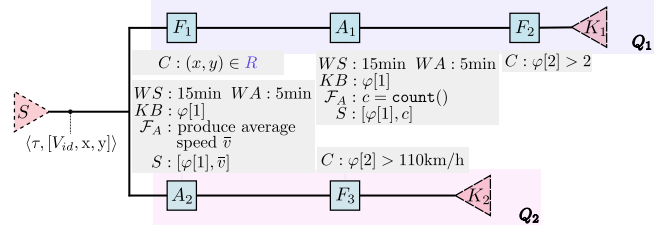


**Figure 3: The DAG of  $Q_1, Q_2$  from Figure 1. Source tuples contain reports' timestamp in  $\mu$ , and the vehicle ID  $V_{id}$  and position  $x, y$  in  $\varphi$ . Source tuples are forwarded to both queries. Tuples arriving at the Sinks correspond to alerts in Figure 1.**

its input streams and forwards its watermark downstream. For an Aggregate or Join  $O_i$ , every time the watermark advances from  $W_i^\omega$  to  $W_i^{\omega'}$ , an output tuple is created for each window maintained by  $O_i$  that has a right boundary less or equal to  $W_i^{\omega'}$ . If multiple results are created, they are emitted in event-time order.

## 2.3 Backward Provenance

*Ananke* aims at extending frameworks that provide backward provenance (§1). Such frameworks [19, 20, 30] rely on *instrumented* operators, i.e., wrappers that add extra functionality to operators. Our contribution can extend any streaming framework providing backward provenance, assuming each sink tuple has additional sub-attributes in  $\mu$  that can be used to retrieve the unique source tuples contributing to it. Such sub-attributes can be pointers to source tuples [30] or IDs identifying source tuples maintained in a dedicated provenance buffer [19, 20]. In the remainder, we rely on a general function `get_provenance` to retrieve backward provenance.

## 3 DEFINITIONS AND GOALS

This section includes the definitions we use to present and prove our contribution's correctness, and a formal statement of our goals.

**DEFINITION 3.1.** *We say a tuple  $t$  contributes directly to another tuple  $t^*$  if an operator produces  $t^*$  based on the processing of  $t$  and write:  $t \rightarrow t^*$ . We then say  $t$  contributes to  $t^*$  and use the notation  $t \rightsquigarrow t^*$  if  $t \rightarrow t' \rightarrow t'' \rightarrow \dots \rightarrow t^*$ . Thus, if  $t \rightarrow t^*$ , then  $t \rightsquigarrow t^*$ .*

From the above, a source tuple  $t_S$  from Source  $S$  contributes to a sink tuple  $t_K$  received by Sink  $K$ , if there is a directed, topologically-sorted path  $S, O_1, \dots, O_i, \dots, O_k, K$  and a sequence of tuples  $t_S = t_0, \dots, t_{i-1}, t_i, \dots, t_k = t_K$ , s.t.  $\forall i = 1, \dots, k$ , where  $t_{i-1}$  and  $t_i$  are input and output tuples of  $O_i$ , and  $t_{i-1} \rightarrow t_i$  for all  $i = 1, \dots, k$ .

**DEFINITION 3.2.** *At time  $\omega$ , tuple  $t$  is active if it can still contribute directly to a tuple produced by an operator. Otherwise,  $t$  is inactive. At time  $\omega$ , tuple  $t$  is alive if it is active or if there is at least one active tuple  $t^*$  such that  $t \rightsquigarrow t^*$ . Otherwise,  $t$  is expired.*

For instance, if a Map produces a tuple  $t_2$  upon ingesting tuple  $t_1$ , the latter is *inactive*, but remains *alive* as long as  $t_2$  is being processed downstream (or as long as  $t_2$  itself is alive). Note that all sink tuples are expired by definition. Using the above, we define the live provenance to be delivered by *Ananke*:



**DEFINITION 3.3.** At time  $\omega$  in the execution of a set of queries  $\mathbb{Q}$ , being  $\mathbb{K}_{\mathbb{Q}}$  the set of  $\mathbb{Q}$ 's Sinks, the live, duplicate-free, bipartite graph forward provenance  $\mathbb{F}(\mathbb{Q}, \omega)$  consists of (1) a set of vertices  $V$ , containing exactly one vertex for each sink tuple forwarded to  $\mathbb{K}_{\mathbb{Q}}$ , and exactly one vertex for each source tuple contributing to any sink tuple forwarded to  $\mathbb{K}_{\mathbb{Q}}$ , (2) a set of edges  $E$ , each edge connecting a sink tuple with its contributing source tuples, and (3) a set of “expired” labels  $L$ , one for each vertex in  $V$  if the tuple it refers to is expired.

Notice that if, at time  $\omega$ , a vertex in  $V$  is alive, then more edges connecting such vertex to other vertices could be found later in the execution of  $\mathbb{Q}$ . In Figure 1c, which shows  $\mathbb{F}(\mathbb{Q}, 8:21)$ , new edges could connect the vertices of tuples not marked as expired to vertices referring to sink tuples that have not yet been produced.

Given the preceding definitions, we now formulate our goals and the necessary requirements to reach these (using prefix R- for the latter). For brevity, we refer to vertices containing a source tuple or a sink tuple as *source vertices* and *sink vertices*, respectively, and use the expression *expired* for tuples and vertices interchangeably.

**Problem formulation.** Being  $\mathbb{B}_{\mathbb{Q}}$  a set of streams delivering  $\mathbb{K}_{\mathbb{Q}}$ 's sink tuples with backward provenance retrievable via attribute  $\mu$ , the goal is to continuously deliver  $\mathbb{F}(\mathbb{Q}, \omega)$ 's  $V$ ,  $E$  and  $L$ , for increasing values of  $\omega$ , as one or multiple streams, to meet the following requirements:

- (R-V) Each vertex referring to a source or a sink tuple is delivered exactly once, by a tuple  $\langle \tau_V, [ID_S, t_S] \rangle$  or  $\langle \tau_V, [ID_K, t_K] \rangle$ , respectively.  $ID_i$  is a unique ID for the vertex associated to  $t_i$ ;
- (R-E) each edge between vertices  $ID_S$  and  $ID_K$  is delivered exactly once by a tuple  $\langle \tau_E, [ID_S, ID_K] \rangle$ , with  $\tau_E$  greater than or equal to the timestamp  $\tau_V$  of the connected vertices; and
- (R-L) an “expired” label is delivered once for each vertex  $ID_i$  by a tuple  $\langle \tau_L, [ID_i] \rangle$ , with  $\tau_L \geq \tau_E$ , for each edge  $E$  adjacent to  $ID_i$ .

For the queries in Figure 1a, Figure 4 shows  $\mathbb{F}(\mathbb{Q}, 8:16)$  and the tuples delivered to update it to  $\mathbb{F}(\mathbb{Q}, 8:22)$ .

While referring to a set of queries  $\mathbb{Q}$  and a set of Sinks  $\mathbb{K}_{\mathbb{Q}}$  for generality, our problem formulation is justified even for a single query with exactly one Source and Sink, because subsequent sink tuples can have overlapping sets of source tuples (as in the example of Figure 1), and each such source tuple still needs to be delivered exactly once and later marked as expired.

**Performance metrics.** For provenance to be practical in real-world applications, its performance overheads need to be small. The efficiency of our solution is evaluated through its overhead on the following metrics:

- **Throughput**, number of tuples a query ingests per unit of time.

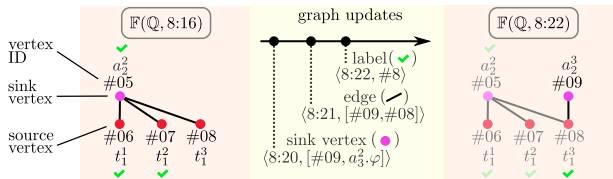


**Figure 4:** Live provenance graph for Figure 1's queries at 8:16 and 8:22, and the stream of graph tuples received in between.

- **Processing Latency**, the delay in the production of a sink tuple after all its contributing source tuples have arrived at the query.
- **CPU utilization**, the percentage of the total CPU time a query utilizes, across all available processors (0-100%).
- **Memory consumption**, the amount of RAM a query utilizes.

We also introduce the *provenance latency* metric, to quantify the event time it takes for  $\mathbb{F}(\mathbb{Q}, \omega)$ 's components to become available:

- For tuple  $t$ 's vertex  $V$ , it is computed as  $\tau_V - t.\tau$ .
- For an edge  $E$ , it is computed as  $\tau_E - \max(\tau_V^S, \tau_V^K)$ , where  $\tau_V^S$  and  $\tau_V^K$  are the timestamps of the vertices connected by the edge.
- For the label  $L$  of some vertex, it is computed as  $\tau_L - \tau_V$ .

**Implementation requirements.** We want *Ananke* to be a streaming-based extension (of  $\mathbb{Q}$ ) that delivers the vertices, edges, and labels of  $\mathbb{F}(\mathbb{Q}, \omega)$  through its output stream(s). A solution can rely on user-defined or native operators (§2). Being a streaming-based extension of  $\mathbb{Q}$ , the latter's watermarks are propagated to *Ananke* operators, too. For generality, we assume a user-defined operator needs to support two methods (not invoked concurrently by the SPE): `on_tuple( $t$ )`, invoked upon reception of tuple  $t$ , and `on_watermark( $W$ )`, invoked when the watermark  $W$  is updated.

## 4 DISCERNING ALIVE AND EXPIRED TUPLES

Live provenance needs to discern alive from expired tuples. Even if sink tuples cannot contribute directly to other tuples, source tuples can be inactive but alive. As we show, alive and expired tuples can be separated using static query attributes and the Sink watermarks.

Figure 5 illustrates how a source tuple's contribution “ripples” through event time for a query composed of Aggregates  $A_1$  and  $A_2$ , Map  $M$ , and Filter  $F$ . A source tuple,  $t_S$ , falls into two windows of  $A_1$ , which emit two outputs that pass through  $M$  and contribute to three separate windows in  $A_2$ . Two of the three output tuples of  $A_2$  get dropped by  $F$ , and a single tuple  $t_K$  arrives at  $K$ . When that happens, it is unknown whether  $t_S$  will contribute to more sink tuples - for example, it is uncertain if  $F$  will drop the next output of  $A_2$ . The figure also explores  $t_S$ 's hypothetical *maximal* contributions: We ignore exact window placements and examine the extreme case, tuples always falling at the beginning or the end of windows. We shade all event times that can contain (direct or

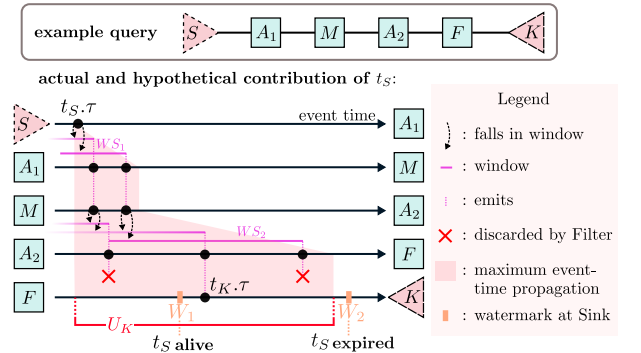


**Figure 5:** Sample query showing actual and maximal contributions of a source tuple to downstream tuples.

indirect) contributions of  $t_S$ . As shown, the growth of the shaded region only depends on the window size of stateful operators. Tuple  $t_S$  can contribute to any tuple inside the shaded region. Thus, if  $K$ 's watermark falls after that region ( $W_2$  in the example), then  $t_S$  is surely expired.  $U_K$  denotes the width of the shaded region. With this intuition, we proceed with proving the following theorem:

**THEOREM 4.1.** *Given  $\mathbb{K}_Q$  (Definition 3.3), it is possible to statically compute constants  $U_K$ , one for each Sink  $K \in \mathbb{K}_Q$  so that: If a source tuple  $t_S$  has contributed to a sink tuple  $t_K$  that arrives at  $K$  at time  $\omega$  or later, then:*

$$t_S.\tau \geq W_K^\omega - U_K. \quad (4.1)$$

*Inversely, if  $t_S.\tau < \min_K (W_K^\omega - U_K)$ , then  $t_S$  is expired and cannot contribute to any sink tuple fed to  $\mathbb{K}_Q$  at time  $\omega$  or later.*

We move bottom-up towards the proof. First, we study pairs of chained operators, each with one downstream peer in Lemma 4.1. In Lemma 4.2, we focus on longer operator chains before examining arbitrary paths between sets of operators in Corollary 4.1 and finally concluding with the proof of Theorem 4.1. Here, we use the term *operator* in a broad sense, also to refer to Sources and Sinks.

**LEMMA 4.1.** *For any operator  $O_i$  with downstream operator  $O_{i+1}$ , and a tuple  $t_{i+1}$  arriving at  $O_{i+1}$  at time  $\omega$  or later, it holds that if an input tuple  $t_i$  of  $O_i$  contributed to  $t_{i+1}$ , then:  $t_i.\tau \geq W_{i+1}^\omega - WS_i$ .*

**PROOF OF LEMMA 4.1.** From the way stateful operators set their output timestamps (§2), we obtain  $t_i.\tau \geq t_{i+1}.\tau - WS_i$ <sup>5</sup>. Furthermore, from Definition 2.1 we get  $t_{i+1}.\tau \geq W_{i+1}^\omega$ . Thus, Lemma 4.1 follows immediately and it also holds for a stateless  $O_i$  by setting  $WS_i = 0$ .  $\square$

We now expand the proof to chains of operators.

**LEMMA 4.2.** *For any chain of operators  $O_1 \dots O_n$ , their downstream operator  $O_{n+1}$  and a tuple  $t_{n+1}$  that arrives at  $O_{n+1}$  at time  $\omega$  or later, it holds that if an input tuple  $t_1$  of operator  $O_1$  contributed to  $t_{n+1}$ , then  $t_1.\tau \geq W_{n+1}^\omega - \sum_{j=1}^n WS_j$ .*

**PROOF OF LEMMA 4.2.** We begin by showing that:

$$\forall t_1, t_{n+1}, \quad t_1 \rightsquigarrow t_{n+1} \Rightarrow t_1.\tau \geq t_{n+1}.\tau - \sum_{j=1}^n WS_j. \quad (4.2)$$

Let us denote as  $t_i$  tuples arriving at operator  $O_i$ , with  $t_i \rightarrow t_{i+1}$  for  $i \in [1, n+1]$ . From the proof of Lemma 4.1, we know that  $t_1.\tau \geq t_2.\tau - WS_1$ . Plugging in this relation again into the first term on the right-hand side of the inequality, we obtain  $t_1.\tau \geq t_2.\tau - WS_1 \geq t_3.\tau - WS_2 - WS_1$ . Performing this step  $n$  times yields Equation 4.2. Given Definition 2.1,  $t_{n+1}.\tau \geq W_{n+1}^\omega$ ; hence:

$$\forall t_1, t_{n+1}, \quad t_1 \rightsquigarrow t_{n+1} \Rightarrow t_1.\tau \geq t_{n+1}.\tau - \sum_{i=1}^n WS_i \geq W_{n+1}^\omega - \sum_{i=1}^n WS_i. \quad \square$$

<sup>5</sup>Although the assumption about how timestamps are set covers commonly used SPEs, the analysis holds also for any output timestamp within the window boundaries. If the output tuples of stateful operator  $O_i$  have timestamps that are  $\Delta_i$  from the left boundary  $L_i$  of the window, it holds that  $t_{i+1}.\tau \leq L_i + \Delta_i$ . By definition of the left boundary, for any tuple  $t_i$  in the window it is true that  $t_i.\tau \geq L_i$  and the relation becomes  $t_i.\tau \geq t_{i+1}.\tau - \Delta_i$ . Since  $WS_i$  is the maximum value of  $\Delta_i$ , using  $WS_i$  will always give correct results (possibly with a higher delay).

**COROLLARY 4.1.** *Given a set of operators  $\mathbb{O} = \{O_i\}$  connected to operator  $O_X$  through a set of paths  $\mathbb{P}$ , for any tuple  $t_X$  fed to  $O_X$  at time  $\omega$  or later, it holds that if an input tuple  $t_i$  of  $O_i$  contributed to  $t_X$ , then  $t_i.\tau \geq W_{out}^\omega - \max_{p \in \mathbb{P}} S_p$  where  $S_p = \sum_{j \in p} WS_j$ .*

The above corollary follows directly from Lemma 4.2 and allows us to compute the maximum “delay” between tuples traversing the longest path in a query, enabling us to prove Theorem 4.1.

**PROOF OF THEOREM 4.1.** To prove Equation 4.1, we apply Corollary 4.1 to any sink tuple  $t_K$  arriving at Sink  $K$  at time  $\omega$  or later, and any source tuple  $t_S$ , which gives  $t_S.\tau \geq W_K^\omega - U_K$ . The constants  $U_K = \max_{p \in \mathbb{P}} S_p$ , with  $\mathbb{P}$  the set of all paths to sink  $K$ , can be computed statically based on the attributes of the query graph.  $\square$

The following remark, stemming directly from Theorem 4.1, introduces a per-application safety-margin for expired tuples.

**REMARK 4.1.** *If we define  $U = \max_K U_K$ , then any source tuple  $t_S$  with  $t_S.\tau < \min_K W_K^\omega - U$  is expired.*

## 5 ALGORITHMIC IMPLEMENTATION

As mentioned in §2, SPEs provide native operators and support user-defined ones. Here we show how *Ananke*'s goals can be met by a user-defined operator (ANK-1, §5.1) or by composing native operators (ANK-N, §5.2). While ANK-1 targets the prompt final labeling of  $\mathbb{F}(\mathbb{Q}, \omega)$ 's vertices, ANK-N shows how the APIs for parallel execution commonly provided by SPEs are sufficient to parallelize *Ananke*'s algorithm. We study their trade-offs in §6.

Both in ANK-1 and ANK-N, the ID of  $t_S$ 's source vertex is based on  $t_S$ 's attributes. Hence, source tuples with equal attributes refer to the same source vertex. As each sink tuple represents a unique event, it results in a sink vertex with a unique ID. Since each sink tuple can carry each source tuple at most once in its provenance, edges are also unique. We discuss in §5.3 how to extend *Ananke* to other ID policies. In the following, we make use of Remark 4.1 for distinguishing alive from expired tuples. As mentioned in §3, the set of streams  $\mathbb{B}_Q$ , delivering backward provenance to *Ananke*, forwards the required watermarks. For both implementations, we show how they meet the requirements for vertices (R-V), edges (R-E), and labels (R-L) from §3.

### 5.1 ANK-1: Single User-defined Operator

As introduced in §3, user-defined operators must support two methods: `on_tuple` and `on_watermark`. Algorithm 1 covers such methods for ANK-1; methods `unique_id()` and `get_id(t)` respectively generate a unique ID and compute the ID of  $t$  based on its attributes.

**CLAIM 5.1.** *A user-defined operator fed  $\mathbb{B}_Q$  can correctly deliver  $\mathbb{F}(\mathbb{Q}, \omega)$  with Algorithm 1's `on_tuple` and `on_watermark` methods.*

**PROOF.** Upon reception of sink tuple  $t_K$  from  $\mathbb{B}_Q$ , ANK-1 emits exactly once the corresponding (1) sink and (2) source vertex, only if its ID was not stored in the timestamp-sorted set  $T$  (i.e., if the corresponding source vertex was not forwarded before), thus meeting requirement (R-V); (3) edges, and (4) sink vertex label (L1-11). Set  $T$  represents ANK-1's “memory” about forwarded source vertices. The emitted tuples carry as timestamp the current watermark value,

```

Data: Set  $T$  of pairs  $(\tau, ID)$ , ordered on  $\tau$ , and watermark  $W$ 

1 Method on_tuple( $t_K$ )
2    $ID_K = \text{unique\_id}()$ ;
3   emit( $\langle W, [ID_K, t_K] \rangle$ ); // Emit sink vertex
4   sourceTuples  $\leftarrow$  get_provenance( $t_K$ );
5   for  $t$ : sourceTuples do
6      $ID_S = \text{get\_id}(t_S)$ ;
7     if  $(t.\tau, ID_S) \notin T$  then
8       emit( $\langle W, [ID_S, t_S] \rangle$ ); // Emit source vertex
9        $T \leftarrow T \cup \{(t.\tau, ID_S)\}$ ;
10      emit( $\langle W, [ID_S, ID_K] \rangle$ ); // Emit edge
11    emit( $\langle W, [ID_K] \rangle$ ); // Emit sink vertex label

2 Method on_watermark( $W$ )
3   for  $(\tau, ID_S) \in T$  do
4     if  $\tau \geq W - U$  then
5       return
6     emit( $\langle W, [ID_S] \rangle$ ); // Emit source vertex label
7      $T \leftarrow T \setminus (\tau, ID_S)$ ;

```

Each source vertex  $ID_S$  in  $T$  is purged once the corresponding source tuple is expired, i.e. when  $W - U$  is greater than its  $\tau_V$  (L12-17). Upon purging of  $ID_S$ , exactly one “expired” label is generated for the corresponding source vertex, with the current watermark as the timestamp. Since watermarks are strictly increasing, it is guaranteed that each label has a timestamp higher than or equal to that of its source vertex, meeting (R-L) for the source vertex.  $\square$

We now present ANK-N, based on native operators. First, we study the case of  $U > 0$ . For ease of exposition, we initially rely on two auxiliary stateful operators, *Delay* (D) and *Forward Once* (FO), that help meet the requirements, and later show how D’s and FO’s semantics can be satisfied by native operators. Finally, we cover the case  $U = 0$ , where all Q’s operators are stateless.

A **Forward Once (FO)** guarantees that, whether one or more tuples are fed to it sharing the same ID sub-attribute, only the earliest such tuple is output, with its payload unchanged but its timestamp delayed by  $\text{delay}()$  as in D. After such tuple is output, FO produces nothing for the subsequent input tuples with that ID until a period of  $U$  has passed in the input stream. As identical source tuples that appear at different times in  $\mathbb{B}_{\mathbb{Q}}$  are not spaced apart further than  $U$  (Remark 4.1) and have the same ID, FO will output unique source tuples exactly once.

Upon processing  $t_K$ ,  $M_u$  produces a sink vertex that carries a copy of  $t_K$ , a unique  $ID_K$  and the character "K" as sub-attributes of its payload.  $M_u$  also produces, for all source tuples in  $t_K$ 's provenance, a source vertex with character "S" (carrying an ID based on the source tuple attributes) as well as an edge. Each edge carries the



CLAIM 5.2. *The DAG in Figure 6, using the D and FO operator, as well as native ones with the mapping function  $M_u$  defined in Algorithm 2, once fed  $\mathbb{B}_{\mathbb{Q}}$ , correctly delivers  $\mathbb{F}(\mathbb{Q}, \omega)$ .*

(1) *Ensuring  $t_S$ 's vertex is created once.*  $t_S$  can appear multiple times, as provenance of multiple sink tuples. Based on Theorem 4.1, after contributing to sink tuple  $t_K$  (timestamped  $\tau_K$ ),  $t_S$  cannot contribute to later sink tuples timestamped  $\geq \tau_K + U$ . Thus, no pair of source tuples with the same ID can be farther away than  $U$ .

(2) *Ordering  $t_S$ 's edges behind the vertex.* For every  $t_S$  in the provenance of  $t_K$ ,  $M_u$  produces the connecting edge "E". For these edges to come after  $t_S$ 's vertex, they are forwarded by  $F_1$  to  $D_1$ , which outputs copies of each edge, with  $\tau_E = \text{delay}(\tau_K)$ , meeting (R-E).

(3) *Producing  $t_S$ 's label correctly.* The latest edge  $E'$  involving  $t_S$  could be produced by  $M_u$  at event time  $\tau_K + U - \epsilon$  (for  $\epsilon > 0$ ), according to Remark 4.1. As  $E'$  will be delayed to  $\tau'_E = \text{delay}(\tau_K + U - \epsilon)$  the source label tuple must be delayed beyond  $\tau'_E$  to meet (R-L). From  $FO$ , the source vertex (which has been delayed already) is multiplexed to  $D_2$ , delayed again, and mapped by  $M_L$  to a label tuple with timestamp  $\tau_{S,L} = \text{delay}(\text{delay}(\tau_K)) = \text{delay}(\tau_K) + 2U$  - which is strictly greater than  $\tau'_E$ , meeting (R-L) for source tuples.

We now focus on sink tuple  $t_K$ 's vertices, edges, and labels:

(2) *Ordering  $t_K$ 's edges behind the vertex.* As explained in (2) above, edges involving  $t_K$  are delayed to  $\tau_E = \text{delay}(\tau_K)$  and (R-E) is met.

(3) *Producing  $t_K$ 's label correctly.* The label for  $t_K$ 's vertex must not

```

1 def  $out = \mathcal{F}_{Mu}(t_K)$ :
2      $ID_K = \text{unique\_id}()$ ;
3      $out.add(["K", t_K, ID_K]);$  // Add sink vertex
4     for  $t_S$  in  $get\_provenance(t_K)$  do
5          $ID_S = \text{get\_id}(t_S)$ ;
6          $out.add(["S", t_S, ID_S]);$  // Add source vertex
7          $out.add(["E", (ID_K, ID_S)]);$  // Add edge
8     return  $out$ ; // Produce tuples

```

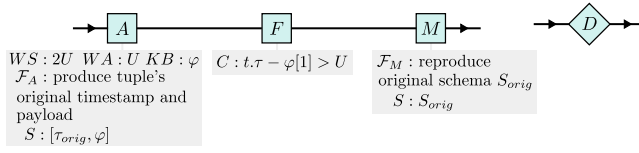


Figure 7: Composition of the D operator.

have a lower timestamp than any edge connected to  $t_K$ 's vertex, and these edges are delayed. As the sink vertex "K" is multiplexed from  $F_2$  to  $D_2$  and mapped to a label by  $M_L$ , the resulting label has timestamp  $\tau_{K,L} = \text{delay}(\tau_K) = \tau_E$ , meeting (R-L) for sink tuples.

Thus, the components involving  $t_K$  also meet the requirements.

Lastly, we now show how Aggregate  $A$  emits vertices, edges, and labels in order. Each tuple, timestamped  $\tau$ , falls in one window  $[\tau, \tau + \delta)$  of  $A$ , and a copy of each tuple is produced by  $A$  when  $A$  receives a watermark  $> \tau + \delta$ . As Aggregates emit results in timestamp-order (§2), this effectively sorts  $A$ 's outputs. Thus, ANK-N correctly delivers live provenance, meeting the requirements in §3.  $\square$

We now construct  $D$  and  $FO$  using native operators:

**Delay.** An Aggregate  $A$ , Filter  $F$  and Map  $M$  (as in Figure 7) can enforce this operator's semantics.  $A$  and  $F$  create the delay, while  $M$  restores the input tuple's payload, creating a delayed copy of it. As  $A$ 's window size is twice as big as its window advance and  $KB : \varphi$ , any input tuple with a unique payload falls into two windows and contributes directly to two output tuples of  $A$ , with timestamps spaced  $U$  apart. As each output tuple  $t^o$  of  $A$  carries the timestamp of its corresponding input tuple ( $\tau_{orig}$ ), the delay induced on the input tuples can be computed as  $t^o.\varphi[1] - t^o.\tau$ .  $F$  ensures that this delay is greater than  $U$ , which is always the case for exactly one of the two tuples produced by  $A$  for each input tuple - the other is delayed at most  $U$  and thus discarded. In the extreme case, an input tuple  $t$  can be delayed by  $A$  by  $2U$  (the window size), namely if  $t.\tau$  coincides with a window's left boundary. The window advance dictates that output tuples produced from  $t$  have timestamps spaced  $U$  apart. Thus, there will also be a tuple delayed by  $U$  produced by  $A$  - however, this tuple will be discarded by  $F$ . This earlier output tuple, in all other cases where  $t$  does not coincide with a window's left boundary, will be delayed even less, and thus also discarded. From this discussion, it is also apparent that the delay for two input tuples  $t_1, t_2 | t_1.\tau = t_2.\tau$  is identical (as both  $t_1$  and  $t_2$  are equally distanced from the left boundaries of the windows they fall in).

**Forward Once.**  $FO$  ensures that from a group of tuples  $t_1, \dots, t_n$  with increasing timestamps, common key  $K$  and  $t_n.\tau - t_1.\tau < U$ , exactly one tuple  $t_{FO}$  with payload  $t_n.\varphi$  is produced. This tuple is delayed from  $t_1$  by at least  $U$  and at most  $2U$ . Figure 8 shows how  $FO$  can be constructed using two Aggregates  $A_1$  and  $A_2$  and a Join  $J$ , to satisfy the required semantics.  $J$ 's predicate is defined as:

$$\text{FOpredicate}(r, s) = ((r.\tau \leq s.\tau) \wedge (r.\varphi[2] \leq s.\varphi[2])) \vee ((s.\tau \leq r.\tau) \wedge (s.\varphi[2] \leq r.\varphi[2])), \quad (5.1)$$

where  $\varphi[2]$  is the count emitted by the Aggregate operators.

The group of input tuples to  $FO$  are multiplexed to both  $A_1$  and  $A_2$ . Since  $t_n.\tau - t_1.\tau < U$ , and the windows of  $A_2$  are offset by  $U$ ,  $t_1, \dots, t_n$  will land in either (1) two windows of one Aggregate and

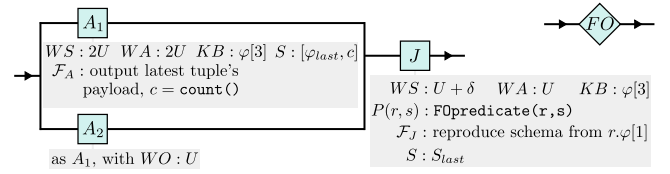


Figure 8: Composition of the FO operator.

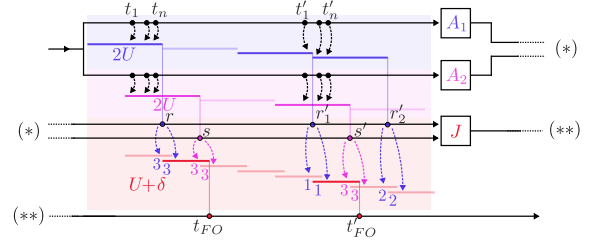


Figure 9: Illustration of how two different groups of input tuples (non-primed and primed) are processed by  $FO$ 's operators. Each group leads to the emission of one tuple.

one window of the other, or (2) in exactly one window in both Aggregates. Figure 9 exemplifies how  $FO$  achieves the required exactly-once forwarding for both cases<sup>6</sup>.  $A_1$  and  $A_2$  produce output tuples that carry the common payload of the input tuples and the count  $c$  of input tuples per window. Their window alignment guarantees that a tuple produced by  $A_1$  or  $A_2$  lands in exactly two of  $J$ 's windows. Let us now explain the two different cases in detail:

- if  $t_1, \dots, t_n$  fall in one  $A_1$  and  $A_2$  window, output tuples  $r$  and  $s$  are then fed to  $J$ . Since  $r.\tau < s.\tau$  and  $r.\varphi[2] = s.\varphi[2]$ , predicate 5.1 holds. When  $J$  emits  $t_{FO}$ , it holds that  $t_1.\tau + U < t_{FO}.\tau \leq t_1.\tau + 2U$ .
- if  $t'_1, \dots, t'_n$  fall in two  $A_1$  windows and one  $A_2$  window, output tuples  $r'_1, r'_2, s'$  are fed to  $J$ . Then, two windows of  $J$  have one tuple each from  $A_1$  and  $A_2$ ; however, predicate 5.1 holds only for the earlier of the two windows, in which  $r$  has lower timestamp and lower count  $c$ . Also in this case,  $t'_1.\tau + U < t_{FO}.\tau \leq t'_1.\tau + 2U$ .

Thus, in both cases, the input is deduplicated and delayed, and the timestamp of the output tuple  $t_{FO}/t'_{FO}$  is given by  $\text{delay}(t_1/t'_1)$ .

**Corner case.** If all operators in  $\mathbb{Q}$  are stateless, then  $U = 0$ . This corner case is not covered by the above implementation of ANK-N, as  $D$  and  $FO$  cannot have  $WS = 0$ . If  $U = 0$ , each sink tuple and its single provenance source tuple have the same timestamp; thus, source tuples are immediately expired once event time passes beyond their timestamp. Each sink tuple will be contributed to by a single source tuple; however, the latter could contribute to several sink tuples. One approach for  $U = 0$  is to replace  $D$  and  $FO$  with identity Maps. The final Aggregate  $A$  will then deduplicate source vertices (and source labels, which could now be duplicated as well), as they share the same payload and fall into the same window.

<sup>6</sup>The case in which  $t_1, \dots, t_n$  fall in one window for both  $A_1$  and  $A_2$  but  $A_1$ 's window ends later than  $A_2$ 's one, and the case in which  $t'_1, \dots, t'_n$  fall in two  $A_2$  windows and one  $A_1$  window are given by "swapping"  $A_1$  and  $A_2$ .



**Listing 1:** Transparently instrumenting a query

```

1 // Provenance decorators highlighted in blue
2 ANK.source(sourceStream)
3 .filter(ANK.filter(t -> t.type() == 0 && t.speed() == 0))
4 .keyBy(ANK.key(t -> t.getKey()))
5 .window(SlidingEventTimeWindows.of(WS, WA))
6 .aggregate(ANK.aggregate(new AverageAggregate()))

```

### 5.3 Extensions

*Ananke* associates each sink tuple with a dedicated sink vertex. Hence, our implementations do not need to deduplicate sink vertices, edges, or sink vertex labels. Modifying *Ananke* to allow distinct sink tuples to refer to the same sink vertex and perform that deduplication is nonetheless trivial, as it simply requires to store the sink vertex IDs which have already been forwarded (ANK-1) or to replace the D operators of Figure 6 with FO operators (ANK-N).

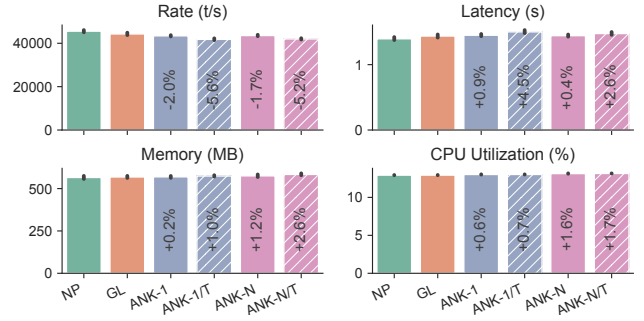
## 6 EVALUATION

We study *Ananke*'s performance relative to the state-of-the-art framework GeneaLog [30]. In §6.1, we compare the performance of queries (1) without provenance, (2) with GeneaLog's backward provenance, and (3) with *Ananke*'s live, forward provenance (ANK-1 and ANK-N, cf. §5). In §6.2, we evaluate the provenance latency for the same use-cases. In §6.3, we compare ANK-1 and ANK-N in-depth, studying their performance for various configurations. Finally, in §6.4 we highlight *Ananke*'s strengths in comparison to ad-hoc implementations relying on tools external to the SPE.

*Ananke Implementation.* *Ananke* is implemented in Java in Flink [8]. It instruments the queries without altering the SPE and uses GeneaLog for backward provenance. We extended GeneaLog to handle tuples arriving at windows of stateful operators out of timestamp order (e.g., when there is parallelism). Moreover, GeneaLog requires operator and tuple objects to *inherit* provenance-specific code. This *non-transparent* (or optimized) implementation can introduce a non-negligible development and maintenance overhead, as implementations need to be altered tying the query implementation to the provenance framework. Here we introduce an alternative *transparent* implementation (denoted by suffix /T), which is based on *encapsulation*: The query is decoupled from the provenance capture, which can be enabled through an automated process. As illustrated in Listing 1, the developer simply encapsulates each Flink operator function with the appropriate framework decorators. Those decorators encapsulate the tuples inside special meta-tuples that contain the provenance metadata populated according to the semantics of the underlying operator function, constructing the provenance graph without user intervention. While more flexible, the extra abstraction layers of this technique can increase the data serialization

**Table 1:** Query configurations explored in the evaluation.

	NP	GL	ANK-1	ANK-1/T	ANK-N	ANK-N/T
Provenance	-	Backward	Live	Live	Live	Live
Native Ops	-	No	No	No	Yes	Yes
Transparent	-	No	No	Yes	No	Yes

**Figure 10:** Performance - Linear Road queries.

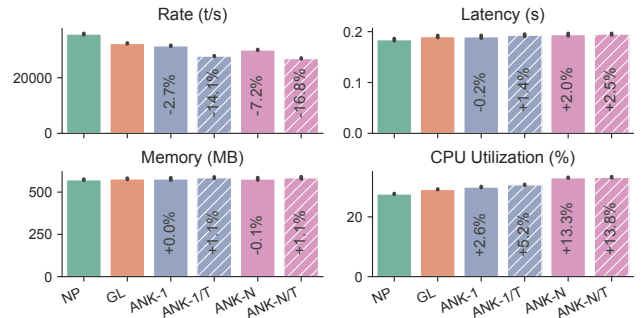
overhead and lower performance. We study both techniques and let the user choose between flexibility and performance.

*Evaluation Setup.* To account for the broad range of modern CPSs' devices, we use (1) Odroid-XU4 [21] devices (or simply *Odroid*), mounting Samsung Exynos5422 Cortex-A15 2Ghz and Cortex-A7 Octa core CPUs, 2 GB RAM, running Ubuntu 18.04.2, OpenJDK 1.8.0\_252, and Flink 1.10.0 (pinned to the four big cores); and (2) a single-socket Intel Xeon-Phi server with 72 1.5GHz cores with 4-way hyper-threading, 32KB L1 and 1MB L2 caches, 102 GB RAM, running CentOS 7.4, OpenJDK 1.8.0\_161, and Flink 1.10.0. The execution environment is made explicit in each experiment.

We study the average *throughput*, *latency*, *CPU* and *memory* utilization (§3). For real-world use-cases (§6.1), we also study the provenance latency. These experiments are repeated at least ten times and are at least ten minutes long. Results are presented as averages with 95% confidence intervals between repetitions. Unless otherwise stated, the parallelism of all operators is set to one. We evaluate the scalability of ANK-N separately in §6.3.

### 6.1 Comparison With the State-of-the-art

To compare with GeneaLog, we study four queries from the domain of CPSs [30], targeting smart highways and smart grids, and four from smart vehicular systems. The latter are real-world examples from the automotive industry, with broader provenance characteristics, more operators, and larger data volumes. To show *Ananke*'s support for multiple Sinks, we run queries from the same

**Figure 11:** Performance - Smart Grid queries.

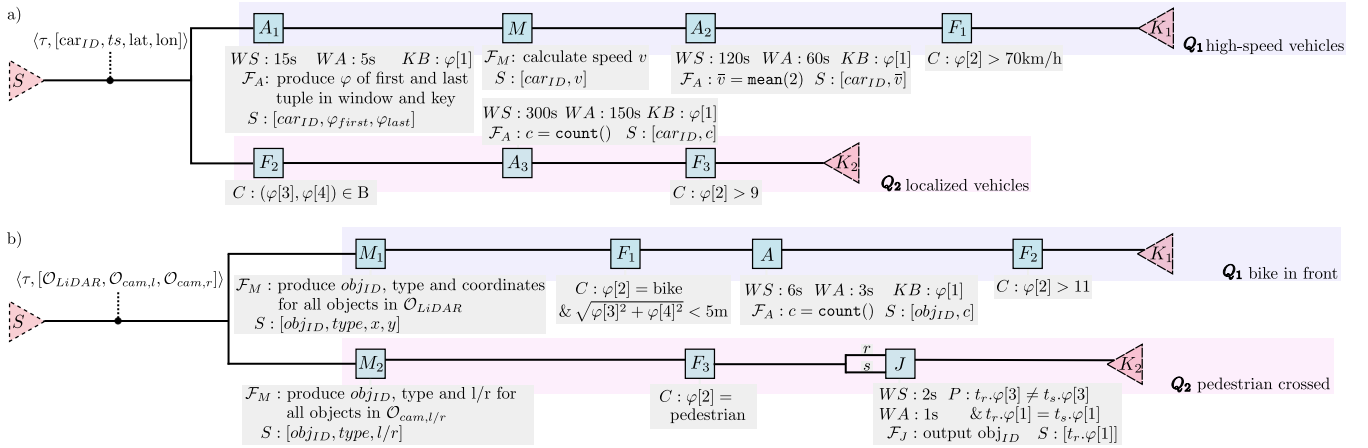


**Figure 12: Real-world example queries: a) Vehicle Tracking queries.**  $\tau$ , lat, lon give the timestamp, GPS latitude and GPS longitude of the car with ID  $car_{ID}$ . b) Object Annotation queries.  $v_L, v_R$  are the camera images from the left- and right-facing camera modules;  $l$  is the LiDAR point cloud.  $obj$  is a concretely-bounded object within an image or a point cloud.

domain together and present the aggregated performance results. Each experiment explores all configurations in Table 1.

**Linear Road.** We run two queries from the Linear Road Benchmark [6] on an Odroid. The first query detects broken-down vehicles through consecutive reports of zero speed and constant position. The second detects accidents from cars stopped at the same position. Both queries receive reports from vehicles every 30 seconds, and contain Aggregates and Filters (we refer the reader to [30] for more details). Each sink tuple depends on 4 source tuples in the first query and 8 in the second. Figure 10 shows the query performance without provenance (NP), with GeneaLog (GL), and *Ananke* with the user-defined operator (ANK-1, ANK-1/T) or the native operators (ANK-N, ANK-N/T). The text in *Ananke*'s bars shows the percentage difference from GL. The performance impact of both GL and *Ananke* is small. GL results in about a 3% performance drop for rate and latency and *Ananke* causes a further drop of 2% for ANK-1 and ANK-N and up to 5.6% for the transparent variants (/T).

**Smart Grid.** Figure 11 shows the performance of two queries from the smart grid domain, run on an Odroid. The first reports long-term blackouts by identifying meters with zero consumption

for 24 hours. The second detects anomalies, through meters that report abnormal consumption at midnight as compensation for the previous day. Both queries receive hourly power measurements and use Aggregates and Filters; the second also has a Join (we refer the reader to [30] for more details). On average, a sink tuple depends on 192 source tuples in the first query and 24 in the second. The provenance overhead is higher here since the queries have larger aggregation windows and higher volumes of provenance data. GL results in a 9% rate drop and 3% latency increase, while ANK-1 (/T) causes a further 2.7% (14.1%) drop in the rate and a jump of 2.6% (5.2%) in the CPU. For ANK-N (/T), the rate drops by 7.2% (16.8%) compared to GL and the latency rises by at most 2.5%, ANK-N's higher number of operators causes a jump in the CPU, around 14%.

**Vehicle Tracking queries.** This use-case is based on Figure 1. It uses the GeoLife dataset, composed of 18670 GPS traces of various vehicles over 4 years around Beijing [41]. We employ 10046 traces of cars driving a full day each to simulate a large fleet driving simultaneously. Figure 12a shows the queries, fed tuples carrying the car ID, timestamp, and latitude/longitude.  $Q_1$  calculates the immediate and average speed of the last two minutes per car, and forwards to  $K_1$  tuples with average speed  $\bar{v} > 70\text{km/h}$ .  $Q_2$  forwards

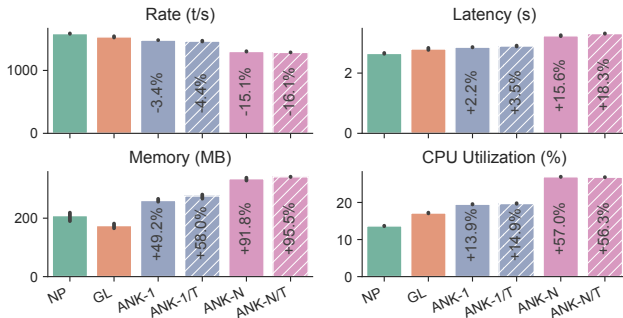


**Figure 13: Performance - Vehicular Tracking queries.**

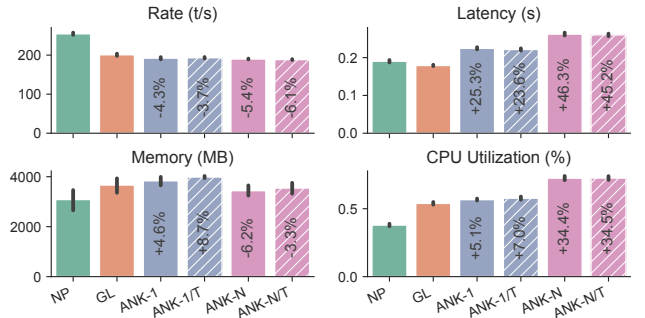


**Figure 14: Performance - Object Annotation queries.**

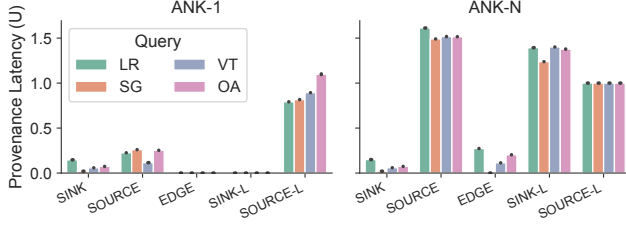


Figure 15: Provenance Latency in multiples of  $U$ .

events with more than 9 coordinates within area  $B$ , a region around Yuyuantan Park in Beijing, to  $K_2$ . This experiment is performed on an Odroid receiving the input data via 100MBit/s Ethernet. Sink tuples of  $Q_1$  depend on around 30-160 tuples and sink tuples of  $Q_2$  depend on 25-250 tuples. As shown in Figure 13, the performance of *Ananke* follows the same trend as before. The impact on rate and latency is small for ANK-1 (/T), at 2-4.5% more than GL and higher for ANK-N (/T), up to 18.3%. The larger provenance graphs of  $Q_1$  and  $Q_2$  cause *Ananke* to have higher resource requirements, with the memory utilization almost doubling in some cases and the CPU utilization jumping by up to 57% in the worst case (ANK-N).

**Object Annotation queries.** These queries enrich an in-vehicle computer vision system based on LiDAR and two cameras. We use the Argoverse Tracking dataset [10], with 113 segments of 15-30s continuous sensor recordings of urban driving, plus 3D annotations of surrounding objects. The two queries, shown in Figure 12b, receive a stream of tuples carrying sets of annotations  $O_{LiDAR}$ ,  $O_{cam,L}$ ,  $O_{cam,R}$ , of objects found by the vehicle’s LiDAR and a left- and right-facing camera. These sets contain objects labeled with the type (e.g., “pedestrian”), 2D position, and a unique object ID.  $M_1$  reproduces all objects found by the LiDAR, while  $F_1$  forwards only bicycles found in front of the vehicle.  $A$  and  $F_2$  then forward a tuple to  $K_1$  if a specific bike was in front of the vehicle for more than 11 frames during a 6s window. In  $Q_2$ , only tuples referring to pedestrians are forwarded as two streams to a Join. If, during 2s, a certain pedestrian is found by both cameras, the pedestrian has crossed, and a tuple is forwarded to  $K_2$ . To simulate powerful, specialized vehicular hardware, this experiment was performed on the Xeon-Phi server. On average,  $Q_1$ ’s sink tuples depend on 15-50 source tuples whereas  $Q_2$ ’s ones depend on 2. The tuples of these queries are much bigger than all previous use-cases, in the order of kilobytes instead of bytes. As evident by the performance of NP in Figure 14, these queries are much more demanding. For example, GL drops 21% in rate, mostly due to the large volume of provenance data transferred between the SPE tasks. *Ananke* has a small effect on the rate, causing a further drop of 3.9-6.6%. Latency is affected more, increasing by about 25% for ANK-1(/T) and 48% for ANK-N(/T), while remaining at small absolute values. Memory consumption does not change significantly compared to GL. The CPU grows for ANK-N(/T), similar to previous use-cases.

## 6.2 Provenance Latency

We now study the provenance latency (§3) for ANK-1 and ANK-N for the Linear Road (LR), Smart Grid (SG), Vehicular Tracking (VT), and Object Annotation (OA) queries. The results are shown

in Figure 15 in multiples of  $U$  (see §5), for vertices (SINK/SOURCE), edges (EDGE), and labels (SINK-L/SOURCE-L) of vertices. As shown, ANK-1 generally has a lower provenance latency than ANK-N. The main difference is that, while ANK-1 can output SOURCE almost immediately (and then store its ID to not output it again), ANK-N delays the production of SOURCE by at least  $U$  to avoid duplicates. This delay propagates to SINK-L (see §5.2). Also, ANK-1 can immediately emit EDGE and SINK-L without any delay (see Algorithm 1). Both variants have low SINK latency as those are safe to emit immediately upon arrival of a sink tuple. The variance is close to zero, as the frequency of watermark updates, the only execution-dependent feature of provenance latency, does not change between repetitions.

## 6.3 ANK-1 vs. ANK-N Trade-offs

Here, we compare ANK-1 and ANK-N for different data characteristics and query configurations. The experiments, run on the Xeon-Phi server, use synthetic queries in which Sources feed *Ananke* (non-transparent) with pre-populated provenance graphs.

Figure 16 shows the performance for different provenance sizes (x-axis) and overlaps (bar colors). The former is the number of source tuples each sink tuple depends on, the latter is the percentage of shared provenance between subsequent sink tuples. ANK-1 has better performance and lower resource requirements than ANK-N, due to the simpler algorithm and single-task deployment. Both ANK-1’s and ANK-N’s performance drops as the provenance size increases, as more data is maintained and transferred between tasks. Larger provenance overlaps result in slightly better performance since fewer source vertices and labels are emitted.

Figure 17 studies ANK-N’s ability to take advantage of the scalability features of the SPE. The x-axis is the number of queries feeding data to *Ananke*, and the bars refer to different parallelism values of *Ananke*. The provenance size is 50, and the overlap 25%. As shown (in log scale), ANK-N outperforms ANK-1 for parallelism 4 or higher since ANK-1 does not support parallel execution. ANK-N’s resource consumption increases with parallelism, making it better suited for use-cases with more available resources. For both

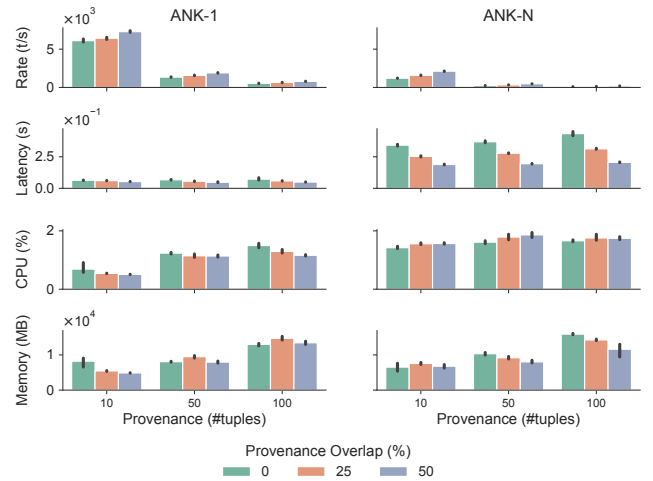


Figure 16: Performance of the synthetic query for different overlaps and provenance sizes.

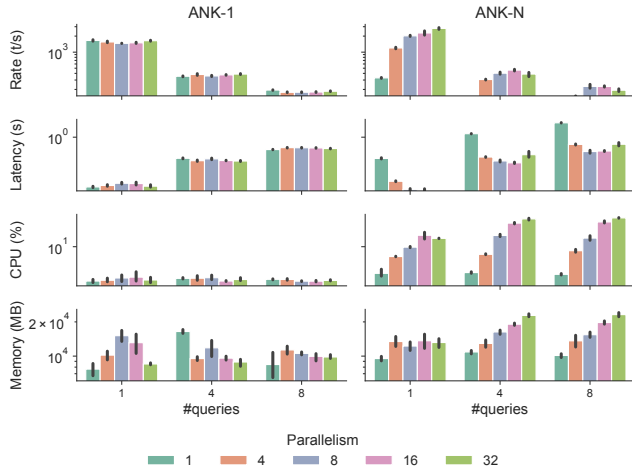


Figure 17: Performance of the synthetic query for different parallelisms and #queries (logarithmic scale).

ANK-1 and ANK-N, a higher number of queries results in a drop in performance, caused by the increased data flow.

#### 6.4 Comparison with On-demand Techniques

ANK-1 and ANK-N are not the only ways to achieve the goals of §3. Here, we compare *Ananke* with ad-hoc alternatives relying on existing systems (external to the SPE) to produce the provenance graph on-demand. These alternatives can seem appealing due to their additional features, e.g. persistent storage of backward provenance. Thus, a comparison with them is crucial to understand the properties of the fully-streaming approach provided by *Ananke*.

We study alternatives based on database systems with varying performance and safety guarantees. The first, SQL-P, relies on an established relational database (PostgreSQL [33]), the second, SQL-I, on a fast, self-contained relational database running *in-memory* (SQLite [35]), and the third, NoSQL, on a non-relational database (MongoDB [27])<sup>7</sup>. The SQL implementations adhere strictly to the goals of §3, whereas NoSQL follows a best-effort principle, without strict ordering guarantees (due to the concurrent accesses by several threads). In contrast with *Ananke*, the alternatives produce the (streaming) provenance graph on-demand. A thread polls the database periodically and performs the data transforms. We evaluate an *aggressive* (suffix /A) polling strategy (as frequently as possible), and a *relaxed* (suffix /R) one (polling every second).

We compare ANK-1 with the above alternatives for two real-world experiments (Smart Grid and Vehicle Annotation queries), as well as for a synthetic one. In addition to previous performance metrics, we also study the *delivery latency* of the provenance graph, to assess the benefits and drawbacks of different polling strategies. This metric expresses the delay (in wall-clock time) between a graph component (vertex, edge, "expired" label) being ready to be delivered and actually being delivered. We do not study memory

<sup>7</sup>A graph database (Neo4J [29]) seems like an obvious choice for provenance data [38], but our preliminary experiments indicated it performed much worse than the alternatives in our streaming applications and is thus not presented here.

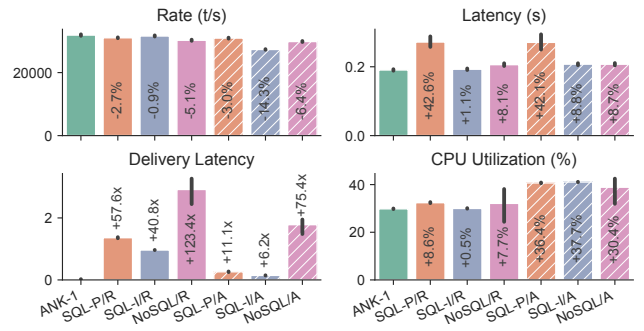


Figure 18: Smart Grid: Performance comparison between *Ananke* and on-demand implementations.

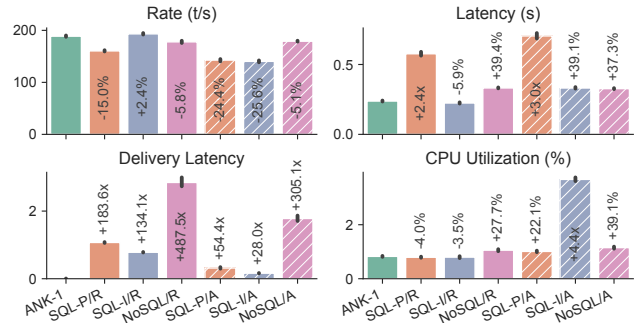


Figure 19: Object Annotation: Performance comparison between *Ananke* and on-demand implementations.

consumption, as the usage of external systems with different storage mechanisms creates a non-uniform measurement environment.

Figures 18 and 19 present the performance of the Smart Grid and Object Annotation queries, respectively. The text inside the bars indicates the relative difference from ANK-1. The performance of the on-demand implementations ranges widely, with relaxed polling (/R) having better rate, latency, and CPU but more than one order of magnitude higher delivery latency. Aggressive polling (/A) lowers the delivery latency but severely degrades the other metrics, in most cases. SQL-I/A achieves the lowest delivery latency (up to 6.2x higher than ANK-1), whereas SQL-I/R has the least impact on the original queries (slightly better rate and latency than ANK-1, at the price of 28x the delivery latency and 4.4x the CPU). SQL-I's implementation closely resembles ANK-1, temporarily maintaining in-memory only unused graph components, instead of persisting all backward provenance data like SQL-P and NoSQL. This similarity in SQL-I's and ANK-1's implementations explains their similarity in performance. NoSQL's best-effort strategy results in a relatively low impact on the original queries but multiple orders of magnitude higher delivery latency than ANK-1, in most cases. SQL-P performs between SQL-I and NoSQL, with lower delivery latency than NoSQL but a much higher impact on the other metrics. This is expected, as SQL-P persists the backward provenance (unlike SQL-I), while also strictly adhering to the goals of §3, in contrast with NoSQL. Both experiments indicate that ANK-1 significantly outperforms all studied alternatives in most or all metrics.



**Table 2: Performance comparison between *Ananke* and on-demand implementations in the synthetic query.**

	ANK-1		SQL-P		SQL-I <sup>*</sup>		NoSQL <sup>*</sup>	
	/R	/A	/R	/A	/R	/A	/R	/A
<b>Rate (t/s)</b>	131.3	54.43	54.80	211.4	209.72	19.81	19.75	
<b>Latency (s)</b>	1.03	2.86	2.82	0.62	0.70	16.19	16.61	
<b>Deliv. Latency (s)</b>	0.07	2.97	0.78	25.10	15.24	27.63	27.29	
<b>CPU (%)</b>	1.18	0.97	1.30	1.75	1.97	0.92	0.89	

<sup>\*</sup> The values for SQL-I and NoSQL do not reflect the steady-state performance, which is significantly lower. Refer to the text for more details.

Table 2 presents the aggregated results of the synthetic experiment, having a setup<sup>8</sup> similar to Figure 16, with a provenance overlap of 0% and provenance sizes 10-100. The relative performance is comparable to the real-world experiments, with ANK-1 outperforming the alternatives overall. SQL-I seems to outperform ANK-1 in rate and latency but a detailed examination of the experimental data indicates that SQL-I can only sustain 40% of the measured rate without exhausting the memory of the system. As, in contrast to ANK-1, the on-demand alternatives lack a back-pressure mechanism, they can fetch backward provenance from the SPE faster than they can process it. This leads to a continuously-increasing provenance backlog (illustrated by the high delivery latencies). For an in-memory database like SQL-I, this is unsustainable<sup>9</sup>. While backpressure could be added manually to the studied alternatives, this would be “reinventing the wheel” as such mechanisms are available out-of-the-box in *Ananke*, running inside the SPE.

Among the studied on-demand alternatives to *Ananke*, SQL-I performs best but is still disadvantaged by not being streaming-oriented. In contrast, ANK-1 has a much better sustained performance and does not have to maintain “raw” provenance. This enables the immediate forwarding of the forward provenance graph stream to a secondary ingesting system without keeping unnecessary state, saving space and computational resources.

*Evaluation summary.* *Ananke* has similar overheads to the state-of-the-art in backward streaming provenance while offering live, forward rather than simply backward provenance. Compared to [30], the best-performing implementations of *Ananke* incur less than 5% drop in the rate in all use-cases and less than 3% increase in latency in all but one use-case. The evaluation shows that *Ananke* is suitable in deployments of real-world applications requiring both efficient processing and live provenance capture. Alternative existing systems fall short in providing the graph timely and in a sustainable fashion suited to the data streaming paradigm.

## 7 RELATED WORK

Data provenance, extensively studied in databases [11, 13, 23], only recently started being in focus in data streaming. Early such work [39] focuses on coarse-grained data stream dependencies. A finer-grained approach, in [40], produces time intervals which *may* contain provenance tuples. [24] focuses on minimizing the storage

<sup>8</sup>For a fair comparison with the on-demand implementations, in this experiment ANK-1 is writing the graph to disk, and thus has a lower performance than in Figure 16.

<sup>9</sup>NoSQL suffers from the same issue; however, in this case, it is less critical since NoSQL does not need to maintain its state in-memory.

requirements of streaming provenance but produces approximate results and lacks support for some native operators (e.g., Join).

To the best of our knowledge, *Ananke* is the first to deliver live forward provenance. [14] presents a system for debugging streaming queries with integrated provenance capture and visualization. However, it focuses on one SPE [17] and slices of the execution (with the option to lazily create the complete query provenance). It requires users to declare relationships between input and output tuples and does not distinguish expired tuples. Likewise, StreamTrace [7], targeting the Trill SPE [9], assists the development and debugging of queries with data visualization, relying on provenance through instrumented operators and ad-hoc query rewriting. *Ananke*’s provenance graph allows creating similar visualizations for the end-to-end system provenance. GeneaLog is the state-of-the-art technique and framework for fine-grained provenance in streaming applications. It records and traces the provenance meta-data while incurring a small, constant per-tuple overhead. In this work, we extend GeneaLog to support out-of-order data and use it as the provider of backward provenance for *Ananke*. Ariadne [19] is a similar framework for fine-grained streaming data provenance using instrumentation. However, it requires variable-length annotations and needs to temporarily store all alive source tuples (including those that do not contribute to any sink tuples) until they become expired. The authors hypothesize the use of static query analysis to discern alive and expired tuples, but without further details. As discussed in §3, *Ananke* can be adjusted for use with Ariadne or any streaming backward provenance framework.

## 8 CONCLUSIONS

We presented *Ananke*, a framework to extend streaming tools for backward-provenance and to deliver a live bipartite graph of fine-grained forward provenance. *Ananke* provides users with richer provenance information, not only specifying which source tuples contribute to which query results, but also whether each source tuple can potentially contribute to future results or not. This distinction can help analysts prioritize the inspection of the large volumes of events commonly observed when monitoring CPSs. We formally prove *Ananke*’s correctness and implement two variations (available in [18]) in Flink. Through our thorough evaluation, we show that *Ananke* incurs small overheads while being able to outperform alternatives relying on tools external to the SPE. Future work can address (1) finer-grained debugging and exploration by expanding *Ananke*’s live provenance to include intermediate tuples produced by query operators, also indicating whether such tuples could contribute to future results, and (2) exploring how *Ananke*’s theoretical foundations about alive/expired tuples can be used in fault-tolerant stream processing.

## ACKNOWLEDGMENTS

Work supported by the Swedish Government Agency for Innovation Systems VINNOVA, proj. “AutoSPADA” grant nr. DNR 2019-05884 in the funding program FFI: Strategic Vehicle Research and Innovation, the Swedish Foundation for Strategic Research, proj. “FiC” grant nr. GMT14-0032, the Swedish Research Council (Vetenskapsrådet) proj. “HARE” grant nr. 2016-03800, and Chalmers Energy AoA framework proj. INDEED and STAMINA.

## REFERENCES

- [1] Tyler Akidau, Alex Balikov, Kaya Bekiroğlu, Slava Chernyak, Josh Haberman, Reuven Lax, Sam McVeety, Daniel Mills, Paul Nordstrom, and Sam Whittle. 2013. MillWheel: fault-tolerant stream processing at internet scale. *Proceedings of the VLDB Endowment* 6, 11 (2013), 1033–1044.
- [2] Tyler Akidau, Robert Bradshaw, Craig Chambers, Slava Chernyak, Rafael J Fer Andez-Moctezuma, Reuven Lax, Sam McVeety, Daniel Mills, Frances Perry, Eric Schmidt, and Sam Whittle Google. 2015. The Dataflow Model: A Practical Approach to Balancing Correctness, Latency, and Cost in Massive-Scale, Unbounded, Out-of-Order Data Processing. *VLDB* 8, 12 (2015), 1792–1803. <https://doi.org/10.14778/2824032.2824076>
- [3] Apache. 2020. Beam. Retrieved November 12, 2020 from <https://beam.apache.org/>
- [4] Apache. 2020. Heron. Retrieved November 12, 2020 from <https://heron.incubator.apache.org/>
- [5] Apache. 2020. Storm. Retrieved November 12, 2020 from <http://storm.apache.org/>
- [6] Arvind Arasu, Mitch Cherniack, Eduardo Galvez, David Maier, Anurag S. Maskey, Esther Ryzkina, Michael Stonebraker, and Richard Tibbetts. 2004. Linear Road: A Stream Data Management Benchmark. In *Proceedings of the Thirtieth International Conference on Very Large Data Bases - Volume 30* (Toronto, Canada) (VLDB '04). VLDB Endowment, Toronto, Canada, 480–491. <http://dl.acm.org/citation.cfm?id=1316689.1316732>
- [7] Leilani Battle, Danyel Fisher, Robert DeLine, Mike Barnett, Badrish Chandramouli, and Jonathan Goldstein. 2016. Making Sense of Temporal Queries with Interactive Visualization. In *Proceedings of the 2016 CHI Conference on Human Factors in Computing Systems - CHI '16*. ACM Press, Santa Clara, California, USA, 5433–5443. <https://doi.org/10.1145/2858036.2858408>
- [8] Paris Carbone, Asterios Katsifodimos, Stephan Ewen, Volker Markl, Seif Haridi, and Kostas Tzoumas. 2015. Apache Flink: Stream and batch processing in a single engine. *Bulletin of the IEEE Computer Society Technical Committee on Data Engineering* 36, 4 (2015), 28–38.
- [9] Badrish Chandramouli, Jonathan Goldstein, Mike Barnett, Robert Deline, Danyel Fisher, John C Platt, James F Terwilliger, and John Wernsing. 2015. Trill: A High-Performance Incremental Query Processor for Diverse Analytics. *VLDB - Very Large Data Bases* 8, 4 (2015), 401–412. <https://doi.org/10.14778/2735496.2735503>
- [10] Ming-Fang Chang, John Lambert, Patsorn Sangkloy, Jagjeet Singh, Slawomir Bak, Andrew Hartnett, De Wang, Peter Carr, Simon Lucey, Deva Ramanan, et al. 2019. Argoverse: 3D Tracking and Forecasting With Rich Maps. In *2019 IEEE/CVF Conference on Computer Vision and Pattern Recognition (CVPR)*. 8740–8749.
- [11] James Cheney, Laura Chiticariu, and Wang-Chiew Tan. 2007. Provenance in Databases: Why, How, and Where. *Foundations and Trends in Databases* 1, 4 (2007), 379–474. <https://doi.org/10.1561/1900000006>
- [12] Daniel Crawl, Jianwu Wang, and Ilkay Altintas. 2011. Provenance for MapReduce-Based Data-Intensive Workflows. In *Proceedings of the 6th Workshop on Workflows in Support of Large-Scale Science* (Seattle, Washington, USA) (WORKS '11). Association for Computing Machinery, New York, NY, USA, 21–30. <https://doi.org/10.1145/2110497.2110501>
- [13] Yingwei Cui, Jennifer Widom, and Janet L. Wiener. 2000. Tracing the Lineage of View Data in a Warehousing Environment. *ACM Transactions on Database Systems* 25, 2 (June 2000), 179–227. <https://doi.org/10.1145/357775.357777>
- [14] Wim De Pauw, Mihai LeŃia, Bugra Gedik, Henrique Andrade, Andy Frenkiel, Michael Pfeifer, and Daby Sow. 2010. Visual Debugging for Stream Processing Applications. In *Runtime Verification*, Howard Barringer, Ylies Falcone, Bernd Finkbeiner, Klaus Havelund, Insup Lee, Gordon Pace, Grigore Roşu, Oleg Sokolsky, and Nikolai Tillmann (Eds.), Vol. 6418. Springer Berlin Heidelberg, Berlin, Heidelberg, 18–35. [https://doi.org/10.1007/978-3-642-16612-9\\_3](https://doi.org/10.1007/978-3-642-16612-9_3)
- [15] Katarina Nielsen Dominiak and Anders Ringgaard Kristensen. 2017. Prioritizing alarms from sensor-based detection models in livestock production - A review on model performance and alarm reducing methods. *Computers and Electronics in Agriculture* 133 (2017), 46 – 67. <https://doi.org/10.1016/j.compag.2016.12.008>
- [16] Romaric Duvignau, Vincenzo Gulisano, Marina Papatriantafillou, and Vladimir Savic. 2019. Streaming Piecewise Linear Approximation for Efficient Data Management in Edge Computing. In *Proceedings of the 34th ACM/SIGAPP Symposium on Applied Computing - SAC '19*. ACM Press, Limassol, Cyprus, 593–596. <https://doi.org/10.1145/3297280.3297552>
- [17] Bugra Gedik, Henrique Andrade, Kun-Lung Wu, Philip S. Yu, and Myungcheol Doo. 2008. SPADE: The System s Declarative Stream Processing Engine. In *Proceedings of the 2008 ACM SIGMOD International Conference on Management of Data (SIGMOD '08)*. Association for Computing Machinery, New York, NY, USA, 1123–1134. <https://doi.org/10.1145/1376616.1376729>
- [18] GitHub. 2020. Ananke Implementation. Retrieved November 12, 2020 from <https://github.com/dmpalyvos/ananke>
- [19] Boris Glavic, Kyumars Sheykh Esmaili, Peter M. Fischer, and Nesime Tatbul. 2014. Efficient Stream Provenance via Operator Instrumentation. *ACM Trans. Internet Technol.* 14, 1, Article 7 (Aug. 2014), 26 pages. <https://doi.org/10.1145/2633689>
- [20] Boris Glavic, Kyumars Sheykh Esmaili, Peter Michael Fischer, and Nesime Tatbul. 2013. Ariadne: Managing Fine-Grained Provenance on Data Streams. In *Proceedings of the 7th ACM International Conference on Distributed Event-Based Systems* (Arlington, Texas, USA) (DEBS '13). Association for Computing Machinery, New York, NY, USA, 39–50. <https://doi.org/10.1145/2488222.2488256>
- [21] HardKernel. 2020. Odroid-XU4. Retrieved November 12, 2020 from <http://www.hardkernel.com>
- [22] Bastian Havers, Romaric Duvignau, Hannaneh Najdataei, Vincenzo Gulisano, Marina Papatriantafillou, and Ashok Chaitanya Koppisetty. 2020. DRIVEN: A framework for efficient Data Retrieval and clustering in Vehicular Networks. *Future Generation Computer Systems* 107 (2020), 1–17.
- [23] Melanie Herschel, Ralf Diestelkämper, and Housseem Ben Lahmar. 2017. A Survey on Provenance: What for? What Form? What From? *VLDB Journal* 26, 6 (2017), 881–906. <https://doi.org/10.1007/s00778-017-0486-1>
- [24] Mohammad Rezwani Huq, Andreas Wombacher, and Peter M.G. Apers. 2011. *Adaptive Inference of Fine-grained Data Provenance to Achieve High Accuracy at Lower Storage Costs*. IEEE Computer Society, USA, 202–209. <https://doi.org/10.1109/eScience.2011.36> eemcs-eprint.21400.
- [25] Jeong-Hyon Hwang, Ugur Cetintemel, and Stan Zdonik. 2007. Fast and Reliable Stream Processing over Wide Area Networks. In *2007 IEEE 23rd International Conference on Data Engineering Workshop*. 604–613. <https://doi.org/10.1109/ICDEW.2007.4401047>
- [26] Jin Li, Kristin Tufte, Vladislav Shkapenyuk, Vassilis Papadimos, Theodore Johnson, and David Maier. 2008. Out-of-order processing: a new architecture for high-performance stream systems. *Proceedings of the VLDB Endowment* 1, 1 (2008), 274–288.
- [27] MongoDB. 2020. MongoDB. Retrieved November 12, 2020 from <https://www.mongodb.com>
- [28] Hannaneh Najdataei, Yiannis Nikolakopoulos, Vincenzo Gulisano, and Marina Papatriantafillou. 2018. Continuous and Parallel LiDAR Point-Cloud Clustering. In *2018 IEEE 38th International Conference on Distributed Computing Systems (ICDCS)*. IEEE Computer Society, Vienna, Austria, 671–684. <https://doi.org/10.1109/ICDCS.2018.00071>
- [29] Neo4j. 2020. Neo4j. Retrieved November 12, 2020 from <https://neo4j.com/>
- [30] Dimitris Palyvos-Giannas, Vincenzo Gulisano, and Marina Papatriantafillou. 2019. GeneaLog: Fine-grained data streaming provenance in cyber-physical systems. *Parallel Comput.* 89 (2019), 102552.
- [31] Dimitris Palyvos-Giannas, Vincenzo Gulisano, and Marina Papatriantafillou. 2019. Haren: A Framework for Ad-Hoc Thread Scheduling Policies for Data Streaming Applications. In *Proceedings of the 13th ACM International Conference on Distributed and Event-Based Systems (DEBS '19)*. ACM, Darmstadt, Germany, 19–30. <https://doi.org/10.1145/3328905.3329505>
- [32] Fabio Pasqualetti, Florian Dörfler, and Francesco Bullo. 2013. Attack Detection and Identification in Cyber-Physical Systems. *IEEE Trans. Automat. Control* 58, 11 (2013), 2715–2729.
- [33] PostgreSQL. 2020. PostgreSQL. Retrieved November 12, 2020 from <https://www.postgresql.org>
- [34] Saeed Salah, Gabriel Maciá-Fernández, and Jesús E. Díaz-Verdejo. 2013. A model-based survey of alert correlation techniques. *Computer Networks* 57, 5 (2013), 1289 – 1317. <https://doi.org/10.1016/j.comnet.2012.10.022>
- [35] SQLite. 2020. SQLite. Retrieved November 12, 2020 from <https://www.sqlite.org/>
- [36] Michael Stonebraker, Ugur Cetintemel, and Stan Zdonik. 2005. The 8 requirements of real-time stream processing. *ACM Sigmod Record* 34, 4 (2005), 42–47.
- [37] Joris van Rooij, Vincenzo Gulisano, and Marina Papatriantafillou. 2018. LoCo-Volt: Distributed Detection of Broken Meters in Smart Grids through Stream Processing. In *Proceedings of the 12th ACM International Conference on Distributed and Event-Based Systems* (Hamilton, New Zealand) (DEBS '18). Association for Computing Machinery, New York, NY, USA, 171–182. <https://doi.org/10.1145/3210284.3210298>
- [38] Chad Vicknair, Michael Macias, Zhendong Zhao, Xiaofei Nan, Yixin Chen, and Dawn Wilkins. 2010. A Comparison of a Graph Database and a Relational Database: A Data Provenance Perspective. In *Proceedings of the 48th Annual Southeast Regional Conference* (Oxford, Mississippi) (ACM SE '10). Association for Computing Machinery, New York, NY, USA, Article 42, 6 pages. <https://doi.org/10.1145/1900008.1900067>
- [39] Nithya N. Vijayakumar and Beth Plale. 2006. Towards Low Overhead Provenance Tracking in Near Real-Time Stream Filtering. In *Provenance and Annotation of Data*, Luc Moreau and Ian Foster (Eds.). Springer Berlin Heidelberg, Berlin, Heidelberg, 46–54.
- [40] Min Wang, Marion Blount, John Davis, Archan Misra, and Daby Sow. 2007. A Time-and-value Centric Provenance Model and Architecture for Medical Event Streams. In *Proceedings of the 1st ACM SIGMOBILE International Workshop on Systems and Networking Support for Healthcare and Assisted Living Environments* (San Juan, Puerto Rico) (HealthNet '07). ACM, New York, NY, USA, 95–100. <https://doi.org/10.1145/1248054.1248082>
- [41] Yu Zheng, Xing Xie, and Wei-Ying Ma. 2010. Geolife: A collaborative social networking service among user, location and trajectory. *IEEE Data Eng. Bull.* 33, 2 (2010), 32–39.